MATHEMATICS AND COMPUTATIONAL SCIENCES

Vol 3(3), 2022, pp:1-10

DOI:10.30511/mcs.2022.554606.1072

ISSN:2717-2708

http://mcs.qut.ac.ir/

Qom University of Technology

A numerical process the mobile-immobile advection-dispersion model arising in solute transport

Y. Esmaeelzade Aghdam [1], B. Farnam [2]

Abstract : In the present article, to find the answer to the mobile-immobile advection-dispersion model of temporal fractional order $0 < \beta \leq 1$ (MI-ADM-TF), which can be applied to model the solute forwarding in watershed catchment and flood, the effective high-order numerical process is gonna be built. To do this, the temporal-fractional derivative of the MI-ADM-TF is discretized by using the linear interpolation, and the temporal-first derivative by applying the first-order precision of the finite-difference method. On the other hand, After obtaining a semi-discrete form, to obtain the full-discrete technique, the space derivative is approximated utilizing a collocation approach based on the Legendre basis. The convergence order of the implicit numerical design for MI-ADM-TF is discussed in that is linear. Moreover, the temporal-discretized structure of stability is also discussed theoretically in general in the article. Eventually, two models are offered to demonstrate the quality and authenticity of the established process.

Keywords: Mobile-immobile advection-dispersion model; Legendre polynomials; Stability; Convergence
2010 Mathematics Subject Classification: 65L60; 97M30; 35R11
Receive: 26 May 2022, **Accepted:** 16 August 2022

1 Introduction

By using physical characteristics or heterogeneity, solute movement in groundwater, rivers, and streams is arranged in distinct ranges. In the past, the advection-dispersion model for the mobileimmobile model or transient storage model has been extensively applied. New studies emphasize its want for more transport models to explain precisely the heterogeneity and connectivity of spatial characteristics in the sense of solute transport from a general network perspective [6, 10]. Breakthrough curves is one of the cases that make these descriptions in karst aquifers and rivers . Subject to occlusion and diversion of the flow induced through in structures including islands and pools, this can display several peaks [7]. Whereas previous methods to explain such difficulties in breakthrough curves included the use of several alternative attitudes but steady model constants can better explain solute transport operations in various reaches. One of these descriptions is the Model mobile-immobile approach. A basic conceptual framework is based on the mobile-immobile strategy: not all opening spaces in a geological medium lead to universal motion. In recent literature of [5], hydrologists have been renowned for the concept of the mobile-immobile for researching transport in saturated and unsaturated areas.

The porous medium transport flow is highly controlled by the advection and dispersion mechanisms (ADM) that anticipate a breakthrough curve. To define the motion of solvent transfer in porous media, the

[1] Corresponding author: Department of Mathematics, Faculty of Science, Shahid Rajaee Teacher Training University, Tehran, 16785 -136, I. R. Iran yonesesmaeelzade@gmail.com
[2] Department of Mathematics, Qom University of Technology, Qom, Iran

ADM is generally used. Increasing evidence shows, nevertheless, that transport in heterogeneous, fractured, and perhaps even homogeneous media becomes hard to understand in the ADM system. Therefore both the ADM and MIM systems complement the Breakthrough Curves and the results indicate that in both porous and fractured media, the MIM model prevails over ADE, particularly to describe the breakthrough curves peaks and long tails [4]. In order to find more information, we recommend the community development projects to previous research [2, 20].

In scientific world for describing mentioned phenomena, fractional derivative processes is used. Fractional derivative processes have many methods that are appealing to the class of solute transport technology. a fundamental principle of numerical method from both the field and micro scales is really the analysis of computational models of solute transport. Fractional scientific models have been exceedingly important and applicable in the fields such as physics, engineering, electromagnetics, chemistry and biology to model natural concepts [14, 17, 3, 18]. Such paper seeks to understand one method focused on derivatives of fractional order.

The numerical computation to solve MI-ADM-TF with $0 < \beta \leq 1$ and $0 < x < 1$ is described in this paper as

$$\mu_1 \frac{\partial v(x,t)}{\partial t} + \mu_2 \mathcal{D}_t^{\beta} v(x,t) = \lambda_1 \frac{\partial^2 v(x,t)}{\partial x^2} - \lambda_2 \frac{\partial v(x,t)}{\partial x} + q(x,t), \quad 0 < t \leq T, \tag{1.1}$$

in which μ_1 and μ_2 are nonnegative and λ_1 and λ_2 are positive. The initial condition of Eq. (1.1) is $v(x,0) = \psi_0(x)$ and the following boundary conditions as

$$v(0,t) = \phi_0(t), \quad v(1,t) = \phi_1(t), \quad t \in [0,T]. \tag{1.2}$$

In the previous equation, the source function is $q(x,t)$, and $\psi_0(x)$, $\phi_0(x)$ and $\phi_1(x)$ are given, and the fractional derivative $\frac{\partial^{\beta} v(x,t)}{\partial t^{\beta}}$ indicates the left Caputo fractional derivative [19] that is described as bellow

$$\mathcal{D}_t^{\beta} v(x,t) = \frac{1}{\Gamma(1-\beta)} \int_0^t (t-\tau)^{-\beta} \frac{\partial v(x,\tau)}{\partial \tau} d\tau, \quad 0 < \beta < 1. \tag{1.3}$$

The left Caputo fractional derivative operator for the polynomial function is also defined as $\mathcal{D}_t^{\beta} t^n = \frac{\Gamma(n+1)}{\Gamma(n+1-\beta)} t^{n-\beta}$.

Many numerical algorithms for solving (1.1) exist, including such: In [12], Liu et al. applied the radial basis scheme to discrete MI-ADM-TF and investigated the numerical analysis In order to model the MI-ADM-TF, Ghehsareh et al. established the meshless system with a step-by-step strategy for temporal derivatives in [8]. The RBF collocation centered on the meshless strategy to solve MI-ADM-TF was introduced by Golbabai et al. [9]. Moreover, the another methods in recent studies is implicit and explicit difference scheme [13, 21, 16] and spectral method [1, 15].

In the prescribed sequence, this study is arranged as

(i) Expanding Collocation Method Based on Legendre Polynomial in Section 2.

(ii) The review of discretization of the temporal-fractional derivative in Section 3.

(iii) Construction a collocation method based on Legendre Polynomial in Section 4.

(iv) Finally, the recommendation and conclusion are expressed in the concluding part.

2 Review of the Discretization Based on Legendre Polynomial

The goal of this part is to introduce the Legendre polynomial to obtain the derivative operator for this basis. We recall that Legendre bases $\mathrm{L}_i(x), i = 0, 1, \ldots$ have been defined by the following recurrence formula on $L_2([-1,1])$ that $\mathrm{L}_0(x)=1,\ \mathrm{L}_1(x)=x$.

$$\mathrm{L}_{i+1}(x)=\frac{2i+1}{i+1}x\mathrm{L}_i(x)-\frac{i}{i+1}\mathrm{L}_{i-1}(x),\quad i=1,2,\ldots.$$

Using Rodrigues' expression $\mathrm{L}_i(x)=\frac{(-1)^i}{2^i i!}\frac{\partial^i(1-x^2)^i}{\partial x^i}$, the Legendre polynomial has the following generalization.

$$\mathrm{L}_i(x)=\frac{1}{2^i}\sum_{r=0}^{\lfloor\frac{i}{2}\rfloor}\frac{(-1)^r(2i-2r)!}{r!(i-r)!(i-2r)!}x^{i-2r}, i=0,1,\ldots. \tag{2.1}$$

With regard to the weight $\frac{2}{2i+1}$, $\mathrm{L}_i(x)$, $i=0,1,\ldots$ are orthogonal polynomials, such that $\langle \mathrm{L}_i(x),\mathrm{L}_j(x)\rangle=\delta_{ij}$, where δ_{ij} is Kronecker delta function. The transposed Legendre polynomials with the change in the dependent variable $x\to 2x-1$ are used to produce this basis in region $[0,1]$ as

$$\mathrm{L}^*_i(x)=\sum_{r=0}^{\lfloor\frac{i}{2}\rfloor}\sum_{\iota=0}^{i-2r}N_{i,r,\iota}x^{\iota}, i=0,1,\ldots, \tag{2.2}$$

where

$$N_{i,r,\iota}=\binom{i-2r}{\iota}\frac{(-1)^{i-r-\iota}2^{\iota-i}(2i-2r)!}{r!(i-r)!(i-2r)!}.$$

Then we conclude that these shifted bases are orthogonal in the interval $[0,1]$. Through using $N+1$-term with $\{\mathrm{L}^*_i(x)\}_{i=0}^{\infty}$, one can approach $v(x,t)\in L_2([0,1])$ as

$$v(x,t)=\sum_{i=0}^{N}a_i\mathrm{L}^*_i(x)=\Lambda\mathrm{L}^T, \tag{2.3}$$

where unknown values and basis functions are represented by vectors $\Lambda_{1\times(N+1)}=[a_0,a_1,\ldots,a_N]$ and $\mathrm{L}_{1\times(N+1)}=[\mathrm{L}^*_0(x),\mathrm{L}^*_1(x),\ldots,\mathrm{L}^*_N(x)]$, respectively. Moreover, the values $a_i, i=0,1,\ldots,N$ have been formulated as having

$$a_i=(2i+1)\int_0^1\mathrm{L}^*_i(x)v(x,t)dx. \tag{2.4}$$

Now, using the said subject for the derivative $\mathrm{L}^*_i(x)$, one can be obtained a full-form in Eq. (2.2) as bellow

$$\frac{\partial^n\mathrm{L}^*_i(x)}{\partial x^n}=\begin{cases}0 & i=0,1,\ldots n-1,\\ \sum_{r=0}^{\lfloor\frac{i}{2}\rfloor}\sum_{\iota=n}^{i-2r}N^n_{i,r,\iota}x^{\iota-n}, & o.w,\end{cases} \tag{2.5}$$

where

$$N^n_{i,r,\iota}=\frac{(-1)^{i-r-\iota}2^{\iota-i}(2i-2r)!}{r!(i-r)!(i-2r-\iota)!(\iota-n)!}.$$

As a consequence, we can indeed be expressed the derivative of function $v(x,t)$ using the formula given as

$$\frac{\partial^n v(x,t)}{\partial x^n}=\sum_{i=0}^{N}a_i\frac{\partial^n\mathrm{L}^*_i(x)}{\partial x^n}=\Lambda\mathfrak{L}^T_n, \tag{2.6}$$

in which $\mathfrak{L}_{\mathfrak{n}1\times(N+1)}=[\frac{\partial^n\mathrm{L}^*_0(x)}{\partial x^n},\frac{\partial^n\mathrm{L}^*_1(x)}{\partial x^n},\ldots,\frac{\partial^n\mathrm{L}^*_N(x)}{\partial x^n}]$ that the vector entries are derived from Eq. (2.5).

Theorem 2.1. *Let $v_N(x,t)$ be the approximation $v(x,t)\in\mathbb{C}^n[0,1]$. Then the approximation $v(x,t)$ uniformly Convergent to $v_N(x,t)$ i.e.*

$$\|v(x,t)-v_N(x,t)\|\le\frac{I^{n+1}}{(n+1)!}M,$$

where the constant I *is* $\max\{1-x_0, x_0\}$ *and* $M = \max_{x\in[0,1]} \frac{\partial^{n+1} v(x,t)}{\partial x^{n+1}}$.

Proof. We use the Taylor expansion for function $v(x,t)$ at a point $x_0 \in [0,1]$ as

$$v(x,t) = v(x_0,t) + (x-x_0)\frac{\partial v(x,t)}{\partial x} + \ldots + \frac{(x-x_0)^n}{n!}\frac{\partial^n v(x,t)}{\partial x^n} + \frac{(x-x_0)^{n+1}}{(n+1)!}\frac{\partial^{n+1} v(\xi,t)}{\partial x^{n+1}},$$

in which $\xi \in [x_0, x]$. Let

$$V(x,t) = v(x_0,t) + (x-x_0)\frac{\partial v(x,t)}{\partial x} + \ldots + \frac{(x-x_0)^n}{n!}\frac{\partial^n v(x,t)}{\partial x^n},$$

then we have

$$|v(x,t) - V(x,t)| = \left|\frac{(x-x_0)^{n+1}}{(n+1)!}\frac{\partial^{n+1} v(\xi,t)}{\partial x^{n+1}}\right|.$$

The best square approximation of $v(x,t)$ can be considered as $v_N(x,t)$. So, one can get

$$\|v(x,t) - v_N(x,t)\|_2 \le \|v(x,t) - V(x,t)\|_2.$$

Using inner product, we get

$$\begin{aligned}\|v(x,t) - v_N(x,t)\|_2^2 \le \|v(x,t) - V(x,t)\|_2^2 &= \int_0^1 |v(x,t) - V(x,t)|^2 dx \\ &= \int_0^1 \Big(\frac{(x-x_0)^{n+1}}{(n+1)!}\frac{\partial^{n+1} v(\xi,t)}{\partial x^{n+1}}\Big)^2 dx \\ &= \left(\frac{I^{n+1}}{(n+1)!}M\right)^2.\end{aligned}$$

The proof is completed. □

3 Discretization of the Temporal-Fractional Derivative

In the current section, we explore how the numerical approach has been used to approach the temporal-fractional derivative. One of the greatest suggestions for temporal derivative discretion is this technique, the finite difference (FD) strategy. Let $\{t_j\}_{j=0}^{M}$, be uniform points with the time step $\delta t = \frac{T}{M}$ in interval $[0,T]$. With the help of the linear scheme defined in the paper [11], the temporal-fractional derivative (1.3) is obtained as the following form

$$\frac{1}{\Gamma(1-\beta)}\int_0^t (t-\tau)^{-\beta}\frac{\partial v(x,\tau)}{\partial \tau}d\tau = \frac{\delta t^{-\beta}}{\Gamma(2-\beta)}\sum_{j=0}^{M} S_{M,j} v(x,t_j) + \mathcal{O}(\delta t^{2-\beta}), \quad 0<\beta<1 \tag{3.1}$$

in which the coefficients $S_{M,j}$ are specified as below

$$S_{M,j} = \begin{cases} 1, & j = M, \\ (M-j-1)^{1-\beta} - 2(M-j)^{1-\beta} + (M-j+1)^{1-\beta}, & 1 \le j < M, \\ (M-1)^{1-\beta} - (M)^{1-\beta}, & j = 0. \end{cases}$$

Lemma 3.1. *(See [11].) Suppose* $v(x,t) \in C^2[0,T]$ *and* $0<\beta<1$*. The error of the approximation to Eq. (3.1) by applying linear scheme is* $\mathcal{O}(\delta t^{2-\beta})$*.*

4 Process of the New Numerical Procedure

In the present section, we demonstrate how to structure a numerical figure to solve MI-ADM-TF. First, with the aid of the fractional derivative of space described in Section 3, we convert Eq. (1.1) into a semi-discrete scheme. Later, with the help of Section 2, we will present a full discrete design to solve this type of equation. Finally, by placing the Collocation points, which are the same as the roots of Legendre polynomial, in a complete discrete design, its linear system is obtained in each time step.
By replacing $\frac{\partial v(x,t)}{\partial t} = \frac{v(x,t_j)-v(x,t_{j-1})}{\delta t} + \mathcal{O}(\delta t), j = 1, 2, \ldots, M$ istead of the time derivative and Eq. (3.1) in (1.1) in lieu of the time fractional derivative, we can get

$$\mu_1 \frac{v(x,t_j) - v(x,t_{j-1})}{\delta t} + \mu_2 \frac{\delta t^{-\beta}}{\Gamma(2-\beta)} \sum_{r=0}^{j} S_{j,r} v(x,t_r) = \lambda_1 \frac{\partial^2 v(x,t_j)}{\partial x^2} - \lambda_2 \frac{\partial v(x,_j)}{\partial x} + q(x,_j) + R^j, \quad j = 1, 2, \ldots, M.$$

where $R^j \leq C\mathcal{O}(\delta t)$ is the truncation error. Denoting $v(x,t_j) = v^j$, $q(x,t_j) = q^j$, $\overline{\mu}_1 = \Gamma(2-\beta)\mu_1$, $\overline{\lambda}_1 = \Gamma(2-\beta)\lambda_1$, $\overline{\lambda}_2 = \Gamma(2-\beta)\lambda_2$ and $\overline{q}(x,t_j) = \Gamma(2-\beta)q(x,t_j)$ and simplifying, we have

$$(\overline{\mu}_1 + \delta t^{1-\beta} \mu_2 S_{j,j}) v^j - \delta t \overline{\lambda}_1 \frac{\partial^2 v^j}{\partial x^2} + \delta t \overline{\lambda}_2 \frac{\partial v^j}{\partial x} = (\overline{\mu}_1 - \delta t^{1-\beta} \mu_2 S_{j,j-1}) v^{j-1} - \delta t^{1-\beta} \mu_2 \sum_{r=0}^{j-2} S_{j,r} v^r + \delta t \overline{q}(x,t_j) + \delta t R^j, \tag{4.1}$$

in which $R^j \leq C\Gamma(2-\beta)\mathcal{O}(\delta t)$. We obtain the approximate implicit discrete scheme by ignoring the term $\delta t R^j$ and indicating V^j as the approximation of v^j, as continues to follow

$$(\overline{\mu}_1 + \delta t^{1-\beta} \mu_2 S_{j,j}) V^j - \delta t \overline{\lambda}_1 \frac{\partial^2 V^j}{\partial x^2} + \delta t \overline{\lambda}_2 \frac{\partial V^j}{\partial x} = (\overline{\mu}_1 - \delta t^{1-\beta} \mu_2 S_{j,j-1}) V^{j-1} - \delta t^{1-\beta} \mu_2 \sum_{r=0}^{j-2} S_{j,r} V^r + \delta t \overline{q}(x,t_j). \tag{4.2}$$

Next, to obtain full-discrete, we will explain precisely the collocation method based on Legendre basis for approximating spatial derivatives.

$$(\overline{\mu}_1 + \delta t^{1-\beta} \mu_2 S_{j,j}) \Lambda^j L^T - \delta t \overline{\lambda}_1 \Lambda^j \mathfrak{L}_2^T + \delta t \overline{\lambda}_2 \Lambda^j \mathfrak{L}_1^T = (\overline{\mu}_1 - \delta t^{1-\beta} \mu_2 S_{j,j-1}) \Lambda^{j-1} L^T - \delta t^{1-\beta} \mu_2 \sum_{r=0}^{j-2} S_{j,r} \Lambda^r L^T + \delta t \overline{q}(x,t_j). \tag{4.3}$$

Now, with the help of the roots of Legendre basis $\{x_p\}_{p=1}^{N-1}$, he upper expression will be decomposed into $N-1$ equations with $N+1$ unknowns. Now, we must have two extra equations. These derive by replacing $v(0,t) = \phi_0(t)$, $v(1,t) = \phi_1(t)$, in (2.3) as the boundary conditions.

$$\sum_{i=0}^{N} a_i^j \mathrm{L}_i^*(0) = \sum_{i=0}^{N} (-1)^i a_i^j = \phi_0(t_j), \qquad \sum_{i=0}^{N} a_i^j \mathrm{L}_i^*(1) = \sum_{i=0}^{N} a_i^j = \phi_1(t_j).$$

So, the system of $N+1$ equations in $N+1$ unknowns is got as below.

$$A\Lambda^j = B\Lambda^{j-1} + Q^j, \quad j = 1, 2, \ldots, M, \tag{4.4}$$

where $Q^j = \delta t[\overline{q}(x_0,t_j), \overline{q}(x_1,t_j), \ldots, \overline{q}(x_{N-1},t_j), 0, 0]^T$, we can be shown the matrix entries of $A_{(N+1)\times(N+1)}$ and $B_{(N+1)\times(N+1)}$ as follows

$$A = [a_{m,n}] = \begin{bmatrix} a_{11} & a_{12} & a_{13} & \cdots & a_{1N} & a_{1(N+1)} \\ a_{21} & a_{22} & a_{23} & \cdots & a_{2N} & a_{2(N+1)} \\ \vdots & \vdots & \vdots & \ddots & \vdots & \vdots \\ a_{(N-1)1} & a_{(N-1)2} & a_{(N-1)3} & \cdots & a_{(N-1)N} & a_{(N-1)(N+1)} \\ 1 & 1 & 1 & \cdots & 1 & 1 \\ 1 & -1 & 1 & \cdots & (-1)^N & (-1)^{N+1} \end{bmatrix}, \tag{4.5}$$

$$B=[b_{m,n}]=\begin{bmatrix} b_{11} & b_{12} & b_{13} & \cdots & b_{1N} & b_{1(N+1)} \\ b_{21} & b_{22} & b_{23} & \cdots & b_{2N} & b_{2(N+1)} \\ \vdots & \vdots & \vdots & \ddots & \vdots & \vdots \\ b_{(N-2)1} & b_{(N-2)2} & b_{(N-2)3} & \cdots & b_{(N-2)N} & b_{(N-2)(N+1)} \\ \phi_0(t_j) & \phi_0(t_j) & \phi_0(t_j) & \cdots & \phi_0(t_j) & \phi_0(t_j) \\ \phi_1(t_j) & \phi_1(t_j) & \phi_1(t_j) & \cdots & \phi_1(t_j) & \phi_1(t_j) \end{bmatrix}, \tag{4.6}$$

in which for $m,n\in\{1,2,\ldots,N+1\}$, we have

$$\begin{cases} a_{mn}=\sum_{r=0}^{\lfloor \frac{m}{2}\rfloor}\Big((\overline{\mu}_1+\delta t^{1-\beta}\mu_2 S_{j,j})\sum_{\iota=0}^{i-2r}N_{m,r,\iota}x_p^{\iota}, -\delta t\overline{\lambda}_1\sum_{\iota=2}^{m-2r}N_{m,r,\iota}^2 x_p^{\iota-2}+\delta t\overline{\lambda}_2\sum_{\iota=1}^{m-2r}N_{m,r,\iota}^1 x_p^{\iota-1}\Big), \\ b_{mn}=(\overline{\mu}_1-\delta t^{1-\beta}\mu_2 S_{j,j-1})\sum_{r=0}^{\lfloor \frac{m}{2}\rfloor}\sum_{\iota=0}^{m-2r}N_{m,r,\iota}x_p^{\iota}-\delta t^{1-\beta}\mu_2\sum_{r=0}^{j-2}\big(S_{j,r}\sum_{r=0}^{\lfloor \frac{m}{2}\rfloor}\sum_{\iota=0}^{m-2r}N_{m,r,\iota}x_p^{\iota}\big). \end{cases} \tag{4.7}$$

We also utilize the initial condition of the problem, $v(x,0)=\psi_0(x)$ integrating with Eq. (2.3), to achieve the initial solution Λ^0 of (4.4) i.e.

$$\Lambda^0=(2i+1)\int_0^1 \mathrm{L}_i^*(x)\psi_0(x)dx, \quad i=0,1,\ldots,N.$$

5 Numerical Problems

For the purpose of showing the sufficiency of the new scheme, we present in this portion the numerical effectiveness of the proposed strategy in two instances. In the temporal parameter, let us take the convergence order $\mathcal{C}_O$ and the rate $\mathcal{C}_R$, respectively as below

$$\mathcal{C}_O=\log_2^{\left(\frac{\|\mathcal{L}_\infty(2\delta t)\|}{\|\mathcal{L}_\infty(\delta t)\|}\right)}, \quad \mathcal{C}_R=2^{\mathcal{C}_O},$$

where $\mathcal{L}_\infty=\max_{j\in\{0,1,\ldots N\}}|V(x_i,T)-v(x_i,T)|$ is the maximum norm error. The algorithm is performed in version 11.2 of Mathematica. the conclusion are created with i7-2630QM CPU 2.00 GHz, RAM 6.00 GB. We also obtain the processor time for the suggested model in order to calculate the computation.

Example 5.1. *Determine the sample as*

$$\begin{cases} \frac{\partial v(x,t)}{\partial t}+\mathcal{D}_t^{\beta}v(x,t)=\frac{\partial^2 v(x,t)}{\partial x^2}-\frac{\partial v(x,t)}{\partial x}+q(x,t), \\ v(0,t)=v(1,t)=0, \quad t\in[0,T), \\ v(x,0)=10x^2(1-x)^2, \quad x\in(0,T), \end{cases}$$

where the source term and the analytical solution are $q(x,t)=(10x^2(1-x^2))(1+\frac{t^{1-\beta}}{\Gamma(2-\beta)})+10(1+t)(-2+14x-18x^2+4x^3)$ *and* $v(x,t)=10(1+t)x^2(1-x)^2$*, respectively.*

The comparison of the absolute error between the methods of [21] is shown in Tables 1 and 2. From these tables, you can look that the error of the new scheme is better than the method of the said paper, and the error of the solution for the current method is convergence to real rate i.e. 2. Moreover, the temporal order of convergence for this example is demonstrated in Table 3 and has been compared with the applied method in [9]. Figure 1 displays the absolute error of approximate solution by using the numerical scheme which shows the results have a low error with increasing time nodes.

Table 1: The comparison the existing method with methods stated in [21] with $M = 100$ for example 5.1 at $T = 1$.

x	*Exact Solution*	*Method of [21] with* $N = 100$		*Current Method with* $N = 5$	
		Numerical Solution	*Absolute Error*	*Numerical Solution*	*Absolute Error*
0.1	0.1620000	0.16184371	$1.56290E{-4}$	0.162090	$8.97155E{-5}$
0.2	0.5120000	0.51059931	$1.40069E{-3}$	0.512181	$1.81417E{-4}$
0.3	0.8820000	0.87902481	$2.97519E{-3}$	0.882262	$2.62325E{-4}$
0.4	1.1520000	1.14770234	$4.29766E{-3}$	1.152320	$3.21829E{-4}$
0.5	1.2500000	1.24502781	$4.97219E{-3}$	1.250350	$3.51850E{-4}$
0.6	1.1520000	1.14719659	$4.80341E{-3}$	1.152350	$3.47206E{-4}$
0.7	0.8820000	0.87818473	$3.81527E{-3}$	0.882306	$3.05973E{-4}$
0.8	0.5120000	0.50972531	$2.27469E{-3}$	0.512230	$2.29847E{-4}$
0.9	0.1620000	0.16127920	$7.20750E{-4}$	0.162125	$1.24512E{-4}$

Table 2: The comparison the error rate of the existing method with [21] for example 5.1 at $T = 1$.

		Method of [21]		*Current Method with* $N = 5$	
M	N	*Absolute Error*	*Error Rate*	*Absolute Error*	*Error Rate*
50	50	$9.4391E{-3}$		$7.07472E{-4}$	
100	100	$5.0134E{-3}$	1.88	$3.51850E{-4}$	2.01072
200	200	$2.5613E{-3}$	1.96	$1.75472E{-4}$	2.00517
400	400	$1.2781E{-3}$	2.00	$8.76250E{-5}$	2.00253

Table 3: The comparison the existing method with methods stated in [9] with $N = 10$ for example 5.1 at $T = 1$.

	Method of [9] for $\beta = 0.4$		*Current Method for* $\beta = 0.4$		*Method of [9] for* $\beta = 0.9$		*Current Method for* $\beta = 0.9$	
M	L_∞	$\mathcal{C}_O$	L_∞	$\mathcal{C}_O$	L_∞	$\mathcal{C}_O$	L_∞	$\mathcal{C}_O$
10	$1.253E{-2}$		$4.15986E{-3}$		$1.053E{-2}$		$1.61746E{-3}$	
20	$6.318E{-3}$	0.9878	$2.02712E{-3}$	1.03711	$5.242E{-3}$	1.0063	$6.79471E{-4}$	1.25125
40	$3.016E{-3}$	1.0668	$1.00266E{-3}$	1.01560	$2.546E{-3}$	1.0402	$3.12546E{-4}$	1.12034
80	$1.423E{-3}$	1.0837	$4.98847E{-4}$	1.00716	$1.237E{-3}$	1.0431	$1.50183E{-4}$	1.05734
160	$7.019E{-4}$	1.0196	$2.48830E{-4}$	1.00343	$6.025E{-4}$	1.0378	$7.36684E{-5}$	1.02761
320	$3.364E{-4}$	1.0611	$1.24270E{-4}$	1.00168	$2.963E{-4}$	1.0239	$3.64932E{-5}$	1.01342

Example 5.2. *Consider the example as*

$$\begin{cases} \frac{\partial v(x,t)}{\partial t} + \mathcal{D}_t^\beta v(x,t) = \frac{\partial^2 v(x,t)}{\partial x^2} - \frac{\partial v(x,t)}{\partial x} + q(x,t), \\ v(0,t) = v(1,t) = 0, \quad t \in [0,T), \\ v(x,0) = x^2(1-x)^2, \quad x \in (0,T), \end{cases}$$

where $v(x,t) = \exp(-t)x^2(1-x)^2$ *and* $q(x,t)$ *are the analytical solution and the source term that is specified by the exact solution, respectively.*

In Table 4, the order and rate convergence of the semi-discrete are demonstrated for $\beta = 0.5$ and $\beta = 0.8$ at $T = 1$ when $N = 7$. From the demonstrated results in this table, we derive that the rate and order of the convergence are related to the actual results. In Fig. 2, the graphs of numerical approximation have been displayed. It is clear from such a diagram that such numerical solution is consistent..

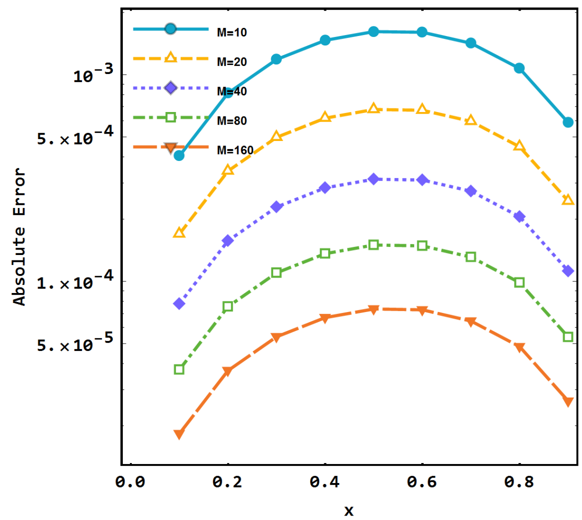

Figure 1: The max absolute error for Example 5.1 with $N = 5$ at $T = 1$.

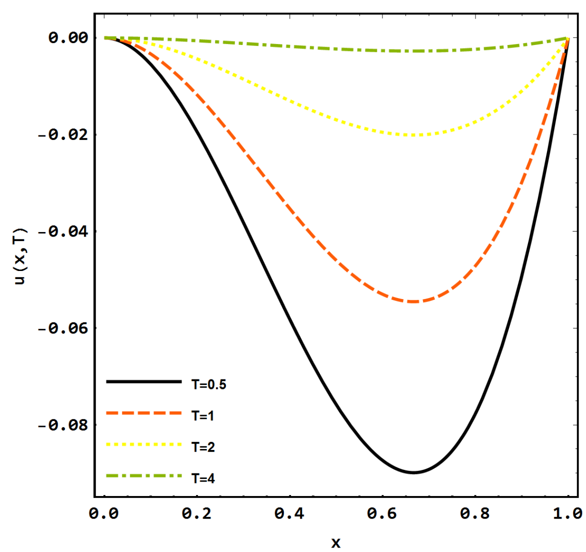

Figure 2: The behavior of the numerical solution for Example 5.2 with $M = 100$, $N = 5$ and $\beta = 0.8$ at $T = 0.5$, $T = 1$, $T = 2$ and $T = 4$.

Table 4: Numerical results of Example 5.2 for $\beta = 0.5$ and $\beta = 0.8$ at $T = 1$ when $N = 7$.

	$\beta = 0.5$					
M	*Max-error*	$\mathcal{C}_O$	$\mathcal{C}_R$	$L_2 - error$	$\mathcal{C}_O$	$\mathcal{C}_R$
10	$3.03721E{-}3$			$6.67365E{-}4$		
20	$1.44431E{-}4$	1.07236	2.10288	$3.17390E{-}4$	1.07222	2.10267
40	$6.97609E{-}4$	1.04989	2.07037	$1.53307E{-}4$	1.04983	2.07029
80	$3.40610E{-}5$	1.03430	2.04812	$7.48539E{-}5$	1.03427	2.04808
160	$1.67531E{-}5$	1.02369	2.03311	$3.68178E{-}5$	1.02367	2.03309
	$\beta = 0.8$					
M	*Max-error*	$\mathcal{C}_O$	$\mathcal{C}_R$	$L_2 - error$	$\mathcal{C}_O$	$\mathcal{C}_R$
10	$4.17527E{-}4$			$9.18322E{-}4$		
20	$1.97839E{-}4$	1.07754	2.11043	$4.35206E{-}4$	1.07730	2.11008
40	$9.45423E{-}5$	1.06530	2.09260	$2.07988E{-}4$	1.06520	2.09246
80	$4.54810E{-}5$	1.0557	2.07872	$1.00058E{-}4$	1.05565	2.07866
160	$2.19921E{-}5$	1.04828	2.06806	$4.83834E{-}4$	1.04826	2.06803

6 CONCLUSION

In this paper, an efficient numerical method to solve the fractional equation (1.1) is investigated. Terms $\frac{\partial v(x,t)}{\partial t}$ and $\mathcal{D}_t^{\beta} v(x,t)$ are discretized with the forward finite difference approach and the linear schemes stated in paper [11] to create a time-discrete approach that yields a semi-temporal form. We have proved that this type of structure is stable by showing the numerical result and established that this method has a convergence order of $\mathcal{O}(\delta t)$. Applying the basis function focused on Legendre polynomials, we proposed a spectral collocation process to obtain a full scheme. The advantage of this strategy is that the offered method's order and stability are well-conditioned for the associated problem to be addressed. We offer that the described computational methods in the current paper would be applied to a kind of different fractional processes.

References

[1] M. Abdelkawy, M.A. Zaky, A.H. Bhrawy, D. Baleanu, Numerical simulation of time variable fractional order mobile-immobile advection-dispersion model, Rom. Rep. Phys, 67(3) 2015, 773-791.

[2] B. Berkowitz, Characterizing flow and transport in fractured geological media: A review, Advances in water resources, 25(8-12) 2002, 861-884.

[3] A. Carpinteri, F. Mainardi, Fractals and fractional calculus in continuum mechanics, Vol. 378, Springer, 2014.

[4] Z. Chen, J. Qian, H. Zhan, L. Chen, S. Luo, Mobile-immobile model of solute transport through porous and fractured media, Proceedings of ModelCARE, 2009 2010, 274.

[5] K. Coats, B. Smith, et al., Dead-end pore volume and dispersion in porous media, Society of petroleum engineers journal, 4(1) 1964, 73-84.

[6] Z. Deng, L. Bengtsson, V.P. Singh, Parameter estimation for fractional dispersion model for rivers, Environmental Fluid Mechanics, 6(5) 2006, 451-475.

[7] M.S. Field, F.J. Leij, Solute transport in solution conduits exhibiting multi-peaked breakthrough curves, Journal of hydrology, 440 2012, 26-35.

[8] H.R. Ghehsareh, A. Zaghian, M. Raei, A local weak form meshless method to simulate a variable order time-fractional mobile-immobile transport model, Engineering Analysis with Boundary Elements, 90 2018, 63-75.

[9] A. Golbabai, O. Nikan, T. Nikazad, Numerical investigation of the time fractional mobile-immobile advection-dispersion model arising from solute transport in porous media, International Journal of Applied and Computational Mathematics, 5(3) 2019, 50.

[10] S. Kim, M.L. Kavvas, Generalized Ficks law and fractional ADE for pollution transport in a river: Detailed derivation, Journal of Hydrologic Engineering, 11(1) 2006, 80-83.

[11] K. Kumar, R.K. Pandey, S. Sharma, Comparative study of three numerical schemes for fractional integro-differential equations, Journal of Computational and Applied Mathematics, 315 2017, 287-302.

[12] Q. Liu, F. Liu, I. Turner, V. Anh, Y. Gu, A RBF meshless approach for modeling a fractal mobile/immobile transport model, Applied Mathematics and Computation, 226 2014, 336-347.

[13] F. Liu, P. Zhuang, K. Burrage, Numerical methods and analysis for a class of fractional advection-dispersion models, Computers & Mathematics with Applications, 64(10) 2012, 2990-3007.

[14] H. Mesgarani, A. Beiranvand, Y.E. Aghdam, The impact of the Chebyshev collocation method on solutions of the time-fractional Black-Scholes, Mathematical Sciences, 2020, 1-7.

[15] H. Pourbashash, Application of high-order spectral method for the time fractional mobile/immobile equation, Computational Methods for Differential Equations, 4(4) 2016, 309-322.

[16] H. Pourbashash, D. Baleanu, M.M. Al Qurashi, On solving fractional mobile/immobile equation, Advances in Mechanical Engineering, 9(1) 2017, 168-178.

[17] H. Safdari, Y. E. Aghdam, J. Gómez-Aguilar, Shifted Chebyshev collocation of the fourth kind with convergence analysis for the space-time fractional advection-diffusion equation, Engineering with Computers, 2020, 1-12.

[18] H. Safdari, H. Mesgarani, M. Javidi, Y.E. Aghdam, Convergence analysis of the space fractional-order diffusion equation based on the compact finite difference scheme, Computational and Applied Mathematics, 39(2) 2020, 1-15.

[19] S. Samuel, V. Gill, On Riesz-Caputo fractional differentiation matrix of radial basis functions via complex step differentiation method, Journal of Fractional Calculus and Applications, 9(2) 2018, 133-140.

[20] H. Scher, M. Lax, Stochastic transport in a disordered solid. I. Theory, Physical Review B, 7(10) 1973, 4491.

[21] H. Zhang, F. Liu, M.S. Phanikumar, M.M. Meerschaert, A novel numerical method for the time variable fractional order mobile-immobile advection-dispersion model, Computers & Mathematics with Applications, 66(5) 2013, 693-701.